Roles of the N- and C-terminal sequences in Hsp27 self-association and chaperone activity

Barbara Lelj-Garolla and A. Grant Mauk*

Department of Biochemistry and Molecular Biology and the Centre for Blood Research, University of British Columbia, Vancouver, BC V6T 1Z3 Canada

Received 3 October 2011; Accepted 31 October 2011
DOI: 10.1002/pro.761
Published online 4 November 2011 proteinscience.org

Abstract: The small heat shock protein 27 (Hsp27 or HSPB1) is an oligomeric molecular chaperone *in vitro* that is associated with several neuromuscular, neurological, and neoplastic diseases. Although aspects of Hsp27 biology are increasingly well known, understanding of the structural basis for these involvements or of the functional properties of the protein remains limited. As all 11 human small heat shock proteins (sHsps) possess an α-crystallin domain, their varied functional and physiological characteristics must arise from contributions of their nonconserved sequences. To evaluate the role of two such sequences in Hsp27, we have studied three Hsp27 truncation variants to assess the functional contributions of the nonconserved N- and C-terminal sequences. The N-terminal variants Δ1–14 and Δ1–24 exhibit little chaperone activity, somewhat slower but temperature-dependent subunit exchange kinetics, and temperature-independent self-association with formation of smaller oligomers than wild-type Hsp27. The C-terminal truncation variants exhibit chaperone activity at 40 °C but none at 20 °C, limited subunit exchange, and temperature-independent self-association with an oligomer distribution at 40 °C that is very similar to that of wild-type Hsp27. We conclude that more of the N-terminal sequence than simply the WPDF domain is essential in the formation of larger, native-like oligomers after binding of substrate and/or in binding of Hsp27 to unfolding peptides. On the other hand, the intrinsically flexible C-terminal region drives subunit exchange and thermally-induced unfolding, both of which are essential to chaperone activity at low temperature and are linked to the temperature dependence of Hsp27 self-association.

Keywords: Hsp27; heat shock proteins; oligomerization; chaperone activity; light scattering; FRET; analytical ultracentrifugation; HSPB1

Introduction

Hsp27 (or HSPB1[1]) is a small heat shock protein (sHsp) that is recognized as a participant in an increasing number of normal and pathological processes. For example, Hsp27 exhibits chaperone activity,[2] inhibits cytochrome *c*-induced apoptosis by inhibiting activation of procaspase-9,[3] modulates oxidative stress and regulates the cytoskeleton.[4–8] In addition, overexpression of Hsp27 by tumor cells increases their tumorigenicity and protects against cell death triggered by a number of stimuli, e.g., hyperthermia, oxidative stress, staurosporine, ligation of the Fas/Apo−1/CD95 death receptor, and cytotoxic drugs.[9] Mutant forms of Hsp27 have been linked to human neuromuscular disorders such as axonal Charcot−Marie−Tooth disease[10,11] and distal hereditary motor neuropathy,[12] and Hsp27 accumulates in individuals with various neurodegenerative disorders, including Alzheimer's, Parkinson's, Alexander's, and Creutzfeldt−Jakob diseases and multiple sclerosis.[13–18]

Grant sponsor: Canadian Institutes of Health Research; Grant number: MCP-14021; Grant sponsor: Canada Research Chair

*Correspondence to: Grant Mauk, Department of Biochemistry and Molecular Biology, Life Sciences Centre, 2350 Health Sciences Mall, University of British Columbia, Vancouver, British Columbia V6T 1Z3, Canada. E-mail: mauk@interchange.ubc.ca

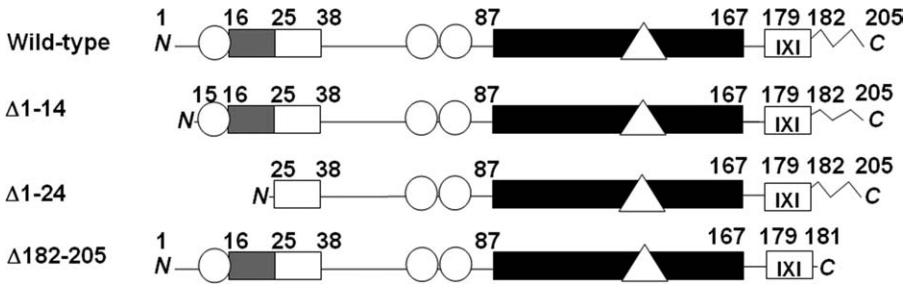

Figure 1. Hsp27 variants studied in this study. The sequence domains of Hsp27 are indicated as follows: Black, conserved α-crystallin domain; dark gray, WDPF-domain; white, conserved N-terminal region; IXI box, conserved IXI sequence at the C-terminus; zigzag line, flexible C-terminal sequence; circles, phosphorylatable seryl residues; triangle, Cys137. Amino acid sequence numbers are indicated above each diagram. The abbreviations used in the text to refer to the various forms of Hsp27 are indicated on the left.

sHsps have been identified in archaea, bacteria, and eukaryotes[19] and are characterized by a low monomeric molecular weight, a conserved α-crystallin domain near the C-terminus, ATP-independent chaperone activity and oligomerization that is regulated by phosphorylation. In addition to the α-crystallin domain, a less conserved domain that is crucial for oligomerization[2,20,21] occurs near the N-terminus and is referred to as the WDPF domain owing to the presence of this sequence of amino acid residues.[22] The variability in the monomeric size of sHsps results primarily from the highly variable N-terminal sequence and from the length of the highly flexible C-terminal sequence.[23] The only conserved sequence near the C-terminus is an IXI/V motif.

Three crystallographically determined structures of sHsps have been reported, and all are from nonmammalian sources. MjHsp16.5 from the thermophile *Methanococcus jannaschii* crystallizes as a 24-mer,[24] and wHsp16.9 from wheat forms a 12-mer.[25] Although both proteins have much shorter N- and C-terminal regions than does Hsp27, they both exhibit chaperone activity. The first structure of an sHsp from a metazoan (a flatworm), Tsp36, reveals the occurrence of monomers with two α-crystallin domains, each preceded by a short N-terminal region, but the protein lacks a flexible C-terminal sequence.[26] More recently, two groups have crystallized truncated forms of Hsp20 and αA-crystallin comprised of the crystallin domain only[27] and forms of αA-crystallin and αB-crystallin comprised of the crystallin domain and part of the C-terminal tail.[28] The latter structures clearly show how the conserved IXI motif interacts with the β4-β8 groove of the α-crystallin domain in more than one conformation.

Although the sHsps share many structural similarities and have highly similar names that imply highly similar functional characteristics, these proteins vary considerably in their functional properties.[1,29] The functional properties of Hsp27 that distinguish it from the other sHsps must arise from contributions provided by the nonconserved regions of the protein. Understanding the mechanisms by which Hsp27 functions, therefore, requires characterization of the self-association, subunit exchange kinetics and chaperone activity of wild-type Hsp27 and that of variant forms of the protein in which the nonconserved regions of the sequence are modified in a systematic manner. In this way, it should be possible to determine the functional relationship of these fundamental properties of the protein with each other and the contributions that specific regions of the protein make toward each of these properties.

We previously reported that human Hsp27 forms a distribution of oligomeric species in which larger oligomers and chaperone activity are favored as temperature is increased.[21,30] Analytical ultracentrifugation experiments performed over a range of Hsp27 concentrations demonstrate clearly that the wild-type protein undergoes a thermally induced increase in oligomeric size from 10 to 40 °C. These larger oligomers are in equilibrium with smaller species, their association is reversible and they are not simply nonspecific aggregates. This study extends this analysis to evaluate the participation of the N- and C-terminal sequences of Hsp27 in the chaperone activity, self–association, and subunit exchange behavior of the protein through characterization of three variants in which these regions of the protein have been truncated (Δ1–14, Δ1–24, Δ182–205) (Fig. 1). The results of this analysis together with the results described above[27,28] are used to propose minimal mechanistic models for Hsp27 chaperone activity and self-association.

Results

Self-association of Hsp27 truncation variants

Self-association of wild-type Hsp27 is temperature-dependent, and oligomer size increases with increasing temperature over the range 10–40 °C.[30] To evaluate the role of the highly conserved N-terminal

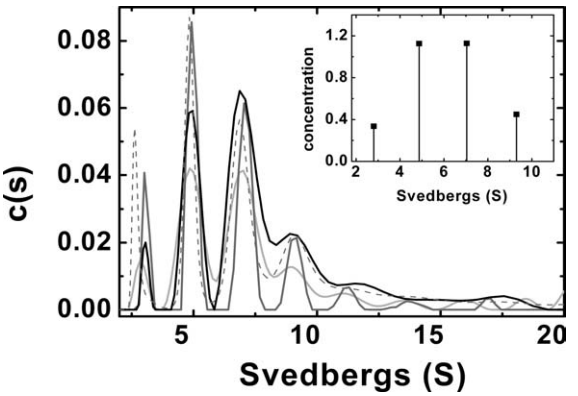

Figure 2. Sedimentation velocity analysis of the Hsp27 Δ1−24 N-terminal deletion variant (Tris−HCl buffer (20 m*M* (pH 8.4), 100 m*M* NaCl)). c(s) distribution: (light gray) 0.4 mg/mL, 40 °C; (dark gray), 0.65 mg/mL, 40 °C; (black), 1.58 mg/mL, 40 °C, (- − -) 1.23 mg/mL, 20 °C. Inset, SEDPHAT analysis for a mixture of dimer, tetramer, hexamer and octamers.

WDPF domain in this temperature dependence, the Δ1−14 Hsp27 variant (which retains the WDPF domain) and the Δ1−24 Hsp27 variant (which lacks the WPDF domain) (Fig. 1) were studied by sedimentation velocity analysis at 40 °C. The behavior of both of these variants at 20 °C was reported previously and established that the lack of a complete N-terminus alters the quaternary structure of the protein by reducing the overall size of the oligomers relative to the wild-type protein.[21] Moreover, results obtained at 20 °C show clearly that the S_{av} of the Δ1−14 variant is consistently greater than that of the Δ1−24 variant at similar concentrations and that self-association of the latter variant is independent of concentration.

Self-association of the Δ1−24 variant as observed by c(s) plots for sedimentation velocity data collected at 40 °C involves discrete speciation that is nearly identical to the behavior observed at 20 °C (Fig. 2) except that a greater fraction (35%) of the protein forms aggregates with sedimentation coefficient between 30 and 150 S rather than oligomers at elevated temperature (data not shown). To identify the oligomeric species of this variant, the high-concentration sample was analyzed with the program SEDPHAT with the "hybrid local continuous distribution and global discrete species" model. The best fit was obtained by fixing the molecular weight of four discrete species corresponding to dimer, tetramer, hexamer, and octamer and allowing the S values to float. The sedimentation coefficient obtained where 2.80 S for the dimer, 4.87 S for the tetramer, 7.04 S for the hexamer, and 9.30 S for the octamers (Fig. 2, insert). A c(s) distribution was included in the fit with S values between 12 and 150 S. The square root of variance was 12 millifringes, and the deviations were randomly scattered.

Similarly, the Δ1−14 variant exhibits comparable speciation at 20 and 40 °C but without the extent of aggregate formation observed for the shorter variant. For this reason, most of our subsequent analysis is focused on the longer ΔN variant. In general, both variants exhibit diminished oligomeric size and more discrete speciation in the c(s) distribution than observed for the wild-type protein at the same temperature (40 °C) (Fig. 2 and Ref. 30). S_{av} values obtained by averaging S in a range where nonspecific aggregation does not occur results in an S_{av} value (40 °C) for the Δ1−14 variant that is greater than that for the Δ1−24 variant, and these values for both variants are less than S_{av} for the wild-type Hsp. This observation is similar to previous results obtained at 20 °C (Table I). Specifically, we previously reported that S_{av} between 1 and 30 S for the Δ1−24 species (0.14 to 1.23 mg/ml) gives a constant value of ~8.5 S. A similar result was observed at 40 °C. The Δ1−14 variant (0.5 mg/ml) exhibits S_{av} (1-30 S) of 10.3 S and a value of 10.6 S at 40 °C (0.55 mg/mL) (Table I). This finding confirms that while the WDPF domain contributes to the formation of larger oligomeric species, the entire N-terminal sequence is required to form oligomers of the size exhibited by wild-type Hsp27 and to enable the change in quaternary structure exhibited by wild-type Hsp27 at elevated temperature (Fig. 3, top panel).

Although small heat shock proteins possess a conserved α-crystallin domain near the C-terminus, the amino acid sequence on the C-terminal side of this domain is highly variable and highly flexible,[23] and its role in self-association is poorly understood. To evaluate possible involvement of this sequence in oligomerization, a variant of Hsp27 lacking the C-terminal 24 amino acids (Δ182−205) (Fig. 1) was prepared. Sedimentation velocity analysis of this variant at 40 °C (Fig. 3) reveals a major component at ~20−22 S and a less abundant, smaller species (3 S). The c(s) plot of this variant at 40 °C also differs slightly from the corresponding plot obtained at 20 °C in that the major peak is more symmetric, but the sedimentation coefficient of the primary sedimenting species at 20 and 40 °C is the same.[21] Thus, self-association of the C-terminal deletion variant is independent of temperature as observed for

Table I. *S_{av} Distribution for Wild-type Hsp27 and N-terminal Deletion Variants*

Protein	*T* (°C)	S_{av}(S)	[Hsp27] (mg/mL)
Wild-type Hsp27	20	12.4	0.5
	40	19.5	0.56
Δ1–14 variant	20	10.3	0.5
	40	10.6	0.55
Δ1–24	20	~8.5	0.14–1.23
	40	~8.4	0.4–1.58

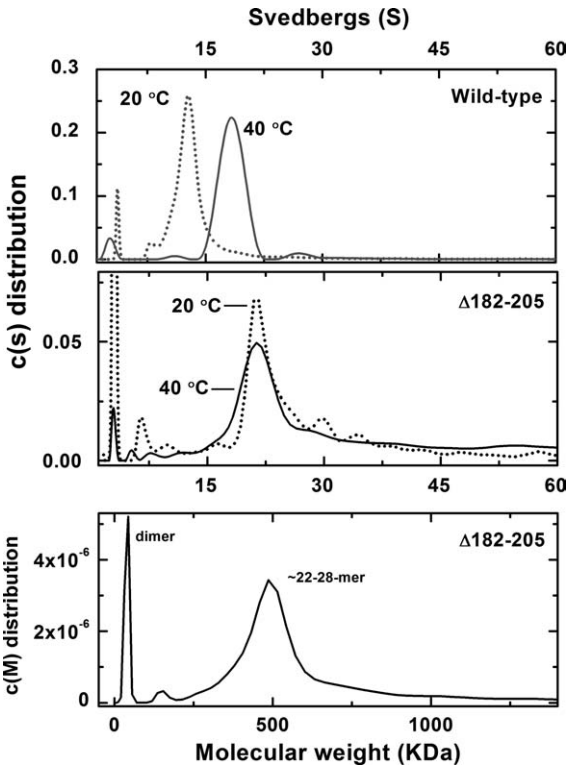

Figure 3. Sedimentation velocity analysis of wild-type Hsp27 (gray) and the Δ182–205 variant (black). Top panel: c(s) distribution of wild-type Hsp27 in Tris−HCl buffer (20 m*M* (pH 8.4), 100 m*M* NaCl); (···) 20 °C (0.50 mg/mL, 22 μ*M*), (——), 40 °C (0.56 mg/mL, 25 μ*M*). Center panel: c(s) distribution of Δ182–205 variant in Tris−HCl buffer (20 m*M* (pH 8.4), 100 m*M* NaCl)), (···) 20 °C (0.38 mg/mL, 19 μ*M*). (——), 40 °C (0.33 mg/mL, 16 μ*M*). Bottom panel: c(M) distribution of the Δ182–205 variant at 40 °C.

the N-terminal deletion variant. However, while the N-terminal deletion variant forms small oligomers at 20 and 40 °C, the C-terminal deletion variant forms primarily large oligomers at both temperatures. Moreover, the c(s) distribution obtained for the Δ182−205 variant at 40 °C is strikingly similar to the plot obtained for the wild-type protein at the same temperature and concentration (Fig. 3). These results indicate that the C-terminus has a significant role in the thermally induced self-association of wild-type Hsp27. A c(M) analysis of the results obtained at 40 °C for the Δ182–205 species indicates that the main sedimenting species has an average molecular weight of 500 kDa, which corresponds to oligomers in the range of 22–28mers (Fig. 3 bottom panel).

Thermal stability

Thermal stability of the wild-type protein was studied between 20 and 95 °C at pH 6.7 and 7.7 [Fig. 4(A)] by circular dichroism. The resulting traces exhibit an unusual shape with ellipticity decreasing linearly with increasing temperature until a sharper decrease is observed between 63 and 70 °C. Previous analytical ultracentrifugation studies of the wild-type protein established that Hsp27 self-associates and that Hsp27 oligomer size increases with temperature in a specific manner.[30] Presumably, the decrease in ellipticity observed before unfolding is related to this tendency of the protein to change quaternary structure prior to unfolding. On the other hand, assuming that the unfolding transition of the monomer is responsible for the abrupt change between 60 and 75 °C, the T_m for wild-type Hsp27 is ~67 °C at both values of pH, which is consistent with values reported previously.[31]

Thermal stability was evaluated by circular dichroism in a similar manner for the Hsp27 truncation variants as shown in Figure 4(B−D). The traces obtained for the Δ182−205 variant indicate that this protein is extremely stable at high temperature [Fig. 4(B)] and at higher pH (7.7) insofar as this variant could not be unfolded completely and did not precipitate even at 99 °C. This behavior may reflect a very stable quaternary structure that limits the ability of individual subunits to unfold.

The unfolding profiles of the Δ1−14 and Δ1−24 variants differ from those observed for all other forms of the protein studied here. Under the conditions studied, both variants exhibit a classic unfolding profile with ellipticity increasing until unfolding is complete, and both proteins denature at high temperatures with formation of a white precipitate [Fig. 4(C−D)]. The larger transition, which may reflect unfolding of the monomer, is similar for the ΔN variants (~67 °C) and for the wild-type protein. These observations are consistent with a role for the N-terminal sequence in Hsp27 self-association, with little or no effect of N-terminal truncation on the stability of the monomer, and with the conclusion that complete unfolding is exhibited only by monomers so that variants with decreased tendency to dissociate (i.e., the C-terminal truncation variant) exhibit greater overall thermal stability than wild-type Hsp27

Chaperone activity

Chaperone activity of the Hsp27 variants was measured by incubating insulin and Hsp27 variants at 20 or 40 °C and by adding DTT to induce insulin unfolding.[30] No scattering is observed in control measurements obtained with Hsp variants alone (i.e., in the absence of insulin), indicating that the signal is attributable solely to the presence of unfolding insulin.

The Δ1−14 variant is nearly devoid of chaperone activity. Any residual activity is essentially independent of protein concentration and is largely unaffected by increasing temperature from 20 to 40 °C [Fig. 5(A,B)]. Similar results were obtained for the Δ1−24 variant (data not shown). The Δ182−205 variant lacks chaperone activity at 20 °C [Fig. 5(A)],

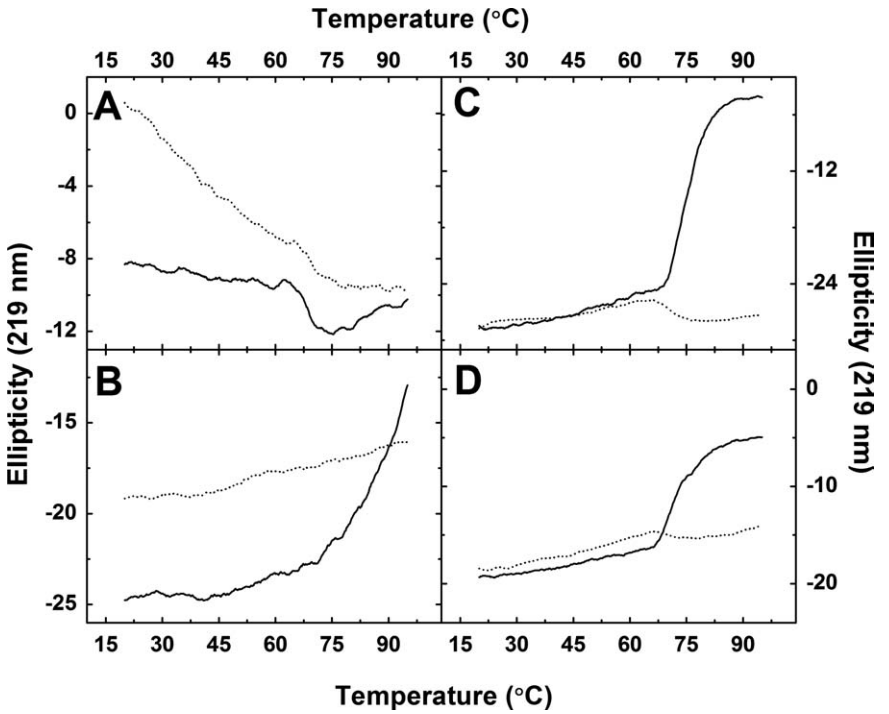

Figure 4. Thermal denaturation of Hsp27 variants monitored by far UV CD. (——), Hsp27 (10 μ*M*) in sodium phosphate buffer (20 m*M*, pH 6.7). (·····), Hsp27 (10 μ*M*) in sodium phosphate buffer (20 m*M*, pH 7.7). A, wild-type Hsp27; B, Δ182−205 Hsp27; C, Δ1−14 Hsp27; D, Δ1−24 Hsp27.

and the rate of turbidity formation increases with addition of this variant to unfolding insulin, presumably owing to the formation of Hsp27−insulin complexes that are larger and/or less soluble than wild-type Hsp27−insulin complexes. A related result in which truncated variants of αA- and αB-crystallin precipitated upon substrate binding to result in increased light scattering has been reported.[28] On heating to 40 °C, however, the Δ182−205 variant does exhibit chaperone activity [Fig. 5(B)]. These results are summarized in Table II along with corresponding data for the wild-type protein.

Subunit exchange

At physiological temperature, mammalian sHsps exhibit a dynamic structure that involves a rapid exchange of subunits between oligomers.[20,32] Although little is known about the mechanism or kinetics of this process, increasing evidence suggests that subunit exchange is essential for chaperone activity.[33–35] To determine if this relationship is also exhibited by Hsp27, the subunit exchange kinetics of wild-type Hsp27 were compared to those of the deletion variants.

The protocol for fluorescence resonance energy transfer (FRET) experiments reported previously to study the subunit exchange kinetics of Hsp27[32,36] was used in this study. In brief two derivatives of Hsp were synthesized by covalently binding either AIAS (4-aceto-4′-((iodoacetyl)amino) stilbene-2,2′-disulfonate) or LYI (luciferase yellow iodoacetamide) to the only free cysteinyl residue of Hsp27 (Cys137). AIAS-modified Hsp27 is a stable derivative with a characteristic fluorescence emission spectrum (λ_{em} = 412 nm) the intensity of which does not change over a 2-h period (data not shown). The rate of change in emission intensity (412 nm) attributable to energy transfer from AIAS to LYI was used to monitor the rate of subunit exchange, and the resulting kinetics traces were fitted (Origin 7.0, OriginLabs) with the simplest model that fit the data well to determine the mean reaction time (t_{mrt}) and the first-order rate constant ($1/t_{mrt}$) for subunit exchange.

The rate of subunit exchange for wild-type Hsp27 increases with increasing temperature [Fig. 6(A), Table III] as observed previously for other small Hsps and α-crystalline,[32,36] and this dependence is consistent with an activation energy of 22.46 kcal/mol at 40 °C and ΔH° of 21 ± 2 kcal/mol. The rate of subunit exchange exhibited by the Δ1−14 variant was generally slower than that of wild-type Hsp27, and the kinetics of exchange were more complex in that the data collected at 20 and 30 °C were fit well with a mono-exponential function but those collected at 37 and 40 °C are better fit to a bi-exponential function owing to the occurrence of a faster exchange process at the higher temperatures. Kinetics parameters were derived from both analyses (Table III), but only the bi-exponential fits are shown [Fig. 6(B)]. The temperature dependent subunit exchange kinetics for the Δ1−14 variant was analyzed in terms of t_{mrt} (20 °C) or t_{mrt1} (30, 37, and

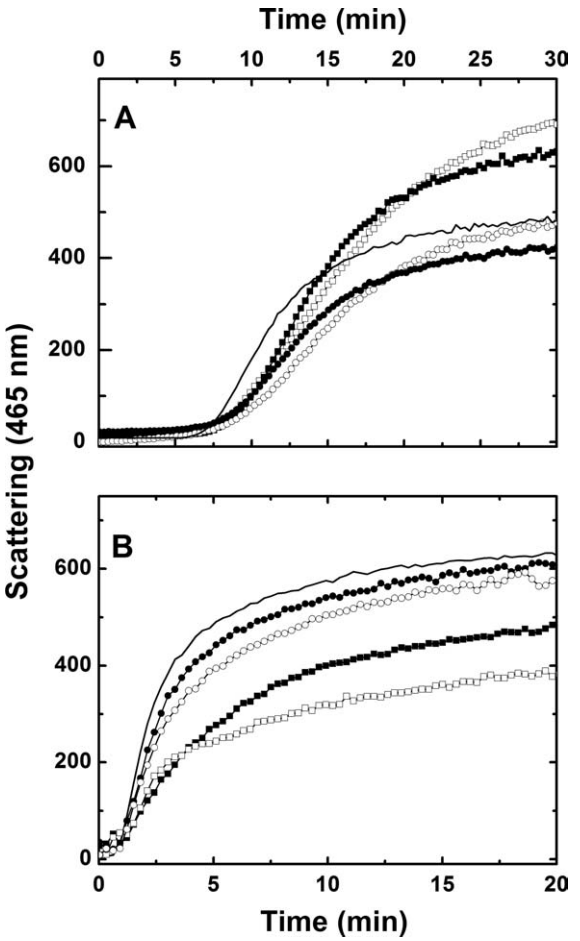

Figure 5. Chaperone activity of Hsp27 variants (sodium phosphate buffer (pH 6.7 (20 m*M*) 100 m*M* NaCl) at (A) 20 °C and (B) 40 °C: (——), DTT-induced aggregation of insulin (40 μ*M*) alone; (●), Δ1–14/insulin (mol/mol), 0.02:1; (○), Δ1–14/insulin (mol/mol), 0.1:1; (■) Δ182–205/insulin (mol/mol), 0.02:1; (□), Δ182–205/insulin (mol/mol), 0.1:1.

40 °C) and was consistent with an activation energy of 26 kcal/mol at 40 °C and ΔH° of 25 ± 6 kcal/mol (data not shown). Because data obtained at 20 °C could be fit as a first order exponential decay, the activation energy and ΔH° were also calculated from the data obtained at 30, 37, and 40 °C by fitting only the values of k_1 obtained from t_{mrt1} (data not shown). In this case, a reaction activation energy of 40.9 kcal/mol at 40 °C and ΔH° of 40.3 ± 6.5 kcal/mol were obtained.

Table II. *Percentage of Inhibition of WT and Variant Forms of Hsp27*

Protein	T (°C)	% inhibition	Insulin:Hsp
Wild-type Hsp27	20	9.3	1:0.05
	40	48.4	
Δ1–14 variant	20	1	1:0.1
	40	7.8	
Δ182–205 variant	20	−43	1:0.1
	40	39	

Inhibition was calculated as $((I_{ins} - I_{ins} + \text{Hsp27})/I_{ins}) \times 100)$ where I is the intensity of light scattering at 30 min (20 °C) or 20 min (40 °C).

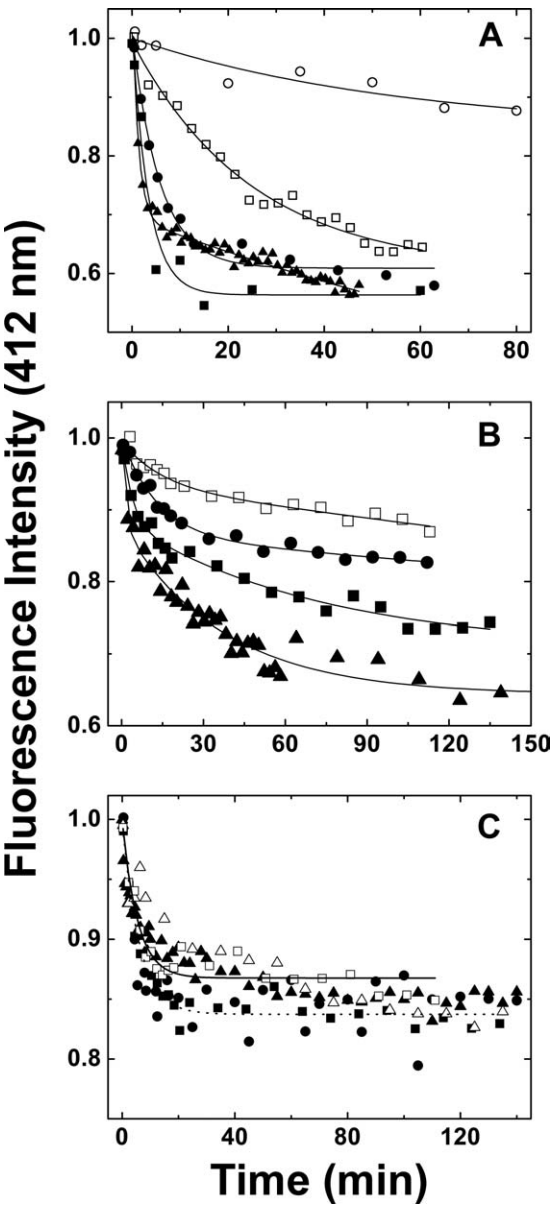

Figure 6. Kinetics of subunit exchange of wild-type Hsp27, the Δ1–14 variant and the Δ182–205 variant as a function of temperature (sodium phosphate buffer (50 m*M*, 100 m*M* NaCl, 2 m*M* DTT, pH 7.5)). Equimolar amounts of AIAS-modified and LYI-modified protein were mixed, and fluorescence emission was monitored (412 nm) at (○) 10 °C; (□) 20 °C; (△), 25 °C; (●) 30 °C, (■) 37 °C, and (▲) 40 °C. (A) Wild-type Hsp27: the curves represent nonlinear regression fits of the data to mono- (10, 20, 30, and 37 °C) or bi-exponential (40 °C) decays. (B) Δ1–14 variant: the curves represent nonlinear regression fits of the data to bi-exponential decays. (C) Δ182–205 variant: the curves represent first to mono-exponential decays for data collected at (——) 20 °C and at (·····) 37 °C.

In general, this variant exhibits slightly slower subunit exchange than does the wild-type protein, and the rate constant for subunit exchange increases with increasing temperature [Fig. 6(B)]. Similar trends have been reported for αA-crystallin in that N-terminal deletion variants exhibit slower

Table III. *Summary of Parameters Derived from Single- and Bi-exponential Decay Fits to Data Obtained for the FRET Experiments with Wild-type and Δ1–14 Hsp27*

	Wild-type Hsp27			Δ1–14 variant						
	$y = y_0 + Ae^{-x/t_{mrt}}$			$y = y_0 + Ae^{-x/t_{mrt}}$			$y = y_0 + A_1e^{(-x/t_{mrt1})} + A_2e^{(-x/t_{mrt2})}$			
T (°C)	t_{mrt} (min)	A	R^2	t_{mrt} (min)	A	R^2	t_{mrt1} (min)	A_1	t_{mrt2} (min)	A_2	R^2
20	22 ± 3	0.39 ± 0.01	0.983	26 ± 5	0.105 ± 0.007	0.941	15 ± 7	0.06 ± 0.02	N/A	N/A	0.957
30	5.8 ± 0.9	0.39 ± 0.01	0.985	18 ± 2	0.160 ± 0.006	0.981	13 ± 5	0.14 ± 0.04	N/A	N/A	0.986
37	3.3 ± 0.5	0.45 ± 0.04	0.964	31 ± 6	0.20 ± 0.01	0.945	4 ± 1	0.12 ± 0.02	70 ± 20	0.18 ± 0.02	0.982
40	1.2 ± 0.1	0.38 ± 0.02	0.984	26 ± 3	0.26 ± 0.01	0.919	1.4 ± 0.8	0.13 ± 0.02	37 ± 4	0.25 ± 0.01	0.958

exchange rates than observed for the wild-type protein, and N-terminal truncation variants from which >50 amino acid residues were deleted showed no chaperone activity, no oligomerization greater than tetramers and no subunit exchange.[37] With sufficiently slow subunit exchange ($k_{off} \leq 10^{-5}$ sec^{-1}) analytical ultracentrifugation should resolve the resulting oligomers as discrete peaks. The results obtained from our FRET experiments are consistent with the analysis that we have proposed for the sedimentation velocity data in the current study.

Interestingly, the first rate constant obtained by fitting the data obtained at high temperature to a bi-exponential decay is very similar to the rate constant obtained for the wild-type protein, so it is difficult to determine which equilibrating oligomeric species are responsible for this first rate constant. Two possibilities are likely: (a) the faster exchange rate constant reflects the dissociation of small oligomers (dimers/tetramers) from larger oligomers as this is the one process that is presumably less affected and limited in the absence of the N-terminal sequence. In this case, the slower exchange rate constant could result from exchange of the intermediate oligomers, i.e. tetramer–octamers and so forth. This slower process is not observed or it is masked in the experiments with the wild-type protein because the presence of the N-terminal tail makes this step much more efficient. (b) Alternatively, smaller oligomers of the N-terminal variant are less efficient overall in exchanging, in which case we are observing the difference between the dimer-oligomer exchange rate (fast) and the monomer–oligomer exchange rate (slow), and this latter process could be masked in the experiments with the wild-type protein.

Despite the temperature dependence of subunit exchange by the Δ1−14 variant, this variant exhibits no chaperone activity. Therefore, the lack of chaperone activity does not result *per se* from the inability to exchange subunits but presumably results from the absence of the critical residues at the N-terminus of the protein that in turn reduces the size of the oligomers accessible to this variant.

In contrast, removal of the C-terminal sequence renders subunit exchange independent of temperature over the range 20–40 °C as indicated by the results obtained for the Δ182−205 variant [Fig. 6(C)]. Analysis of the kinetics data at 20 and 37 °C in terms of a mono-exponential decay is also shown. The resulting t_{mrt1} values were 5.4 ± 0.9 min ($k = 3.1 \times 10^{-6}$ s^{-1}) (20 °C) and 6.0 ± 0.6 min ($k = 2.8 \times 10^{-6}$ s^{-1}) (37 °C). It appears that at all temperatures, the rate of subunit exchange for this variant is similar to that of the wild-type protein at 30−37 °C. Interestingly, the total fluorescence quenching observed for this variant was not as great as observed for the wild-type protein. While the basis for this observation is not readily apparent, it is possible that only some of the protein

undergoes subunit exchange or that the geometry of subunit assembly by the wild-type protein and the Δ182−205 variant differs.

Overall, the complexity of the self-association equilibria exhibited by Hsp27 and these variants limits the extent to which the exact equilibria being monitored in these experiments (e.g., subunit exchange within a small oligomer, exchange of small oligomers with larger assemblies, exchange of monomers or dimers with larger oligomers) can be differentiated.

Discussion

Hsp27 exhibits remarkable versatility in its ability to form oligomers of varying size, to bind a wide range of unfolding substrates, and to recognize specific, folded proteins,[7,8] yet detailed, structure-based mechanisms for these functional properties and their relationships to each other have not been developed. This study is an effort toward that goal that is based on correlating the oligomeric state of the protein with its chaperone activity and subunit-exchange kinetics to define the functional contributions of the N- and C-sequences of the protein. The importance of these regions of small heat shock proteins has been widely recognized and studied in both metazoan[27,28,37–48] and bacterial heat shock proteins.[35,49,50]

This study examines the mechanistic role of the N- and C-terminal sequences of human Hsp27 in the temperature-dependent self-association and in the chaperone activity of the protein. While these two properties of Hsp27 are related,[30] they are not equivalent. Therefore, deletion variants of Hsp27 were analyzed in terms of the temperature dependence of their self-association, their chaperone activities, and their subunit exchange kinetics to determine the extent to which the N- and C-terminal sequences of the protein contribute to these fundamental properties. Results from these studies form the basis for initial models for Hsp27 self-association and chaperone activity as summarized below.

A model for Hsp27 self-association

The N-terminal sequence and the WDPF domain of small heat shock proteins are known to participate in self-association. For example, the N-terminal region of wHsp16.9 is buried in the center of the dodecameric oligomer,[25] and the Tsp36 chaperone forms dimers that are held together by interactions of N-terminal helices.[26] Similarly, deletion of residues 5−23 from Chinese hamster Hsp27 limits self-association to formation of dimers,[22] and the Δ1−14 and Δ1−24 deletion variants of human Hsp27 form oligomers smaller than those observed for the wild-type protein at 20 °C.[30] N-terminal deletion variants of Hsp20, αA- and αB-crystallin exhibit a shift in equilibrium towards smaller oligomers that allowed crystallization and structure determination of the truncated variants.[27,28]

We now find that the Δ1−14 and Δ1−24 variants do not exhibit the temperature dependent self-association (Fig. 2) characteristic of the wild-type protein (Fig. 3 and Ref. 30). Nevertheless, the rate of subunit exchange exhibited by the Δ1−14 variant remains directly proportional to temperature, so although these residues are required for formation of larger oligomers and for thermally-induced self-association, they are not required for efficient dissociation and reassociation through the α-crystallin domain, the C-terminal tail, and whatever remains of the N-terminal regions. This N-terminal region of the sequence has been predicted to form an amphipathic helix[39] as observed for the corresponding region of Tsp36. It seems likely that the N-terminal sequence provides an exposed helical structure that promotes self-association. As this sequence is shortened, the α-crystallin domains become closer to the core of the assembly, fewer oligomeric states are possible, and thermally-induced oligomerization is eliminated. Thus, the size of Hsp27 oligomers varies in the order wild-type (40 °C) > wild-type (20 °C) > Δ1−14 variant (20, 40 °C) > Δ1−24 variant (20, 40 °C) (Table I).

The IXI/V motif (residues 179−181) that occurs toward the *C*-terminus of the protein is highly conserved among small heat shock proteins from protozoans to metazoans, and in the structures of MjHsp16.5 and wHsp16.9, it interacts with the β4−β8 groove in the α-crystallin domain. While the thermophilic Hsp forms these interactions with the C-terminus in just one orientation, this region of the wheat protein exhibits two alternative conformations.[24,25] Tsp36 lacks an extended C-terminal tail, and the IXI/V motif, which binds the hydrophobic groove at the β4−β8 interface, is present at the N-terminus (Ile3, Pro5). More interestingly, crystallographic characterization of a fragment of α-crystallin that retains most of the C-terminal sequence clearly demonstrates binding of the IXI motif of this protein in two orientations to a groove at the β4−β8 interface with observation of more than one domain swap arrangement.[28] These findings indicate that interaction of the IXI motif with the β4−β8 groove in the α-crystallin domain is important for assembly of higher order oligomers and for polydispersity.

The similarity of Hsp27 and α-crystallin permits speculation that the IXI motif of Hsp27 binds in a fashion similar to that observed in the structure of the α-crystallin domain while the role of the flexible hinge that occurs on the N-terminal side of the IXI motif allows the C-terminal tail to accommodate bidirectional binding. Two questions remain: What is the role of the 24 C-terminal residues (Pro182−Lys205), and to which subunit does each IXI motif bind in Hsp27? The flexible C-terminal sequence that follows the conserved IXI region of human Hsp27 is longer (24 residues) than that of MjHsp16.5 (1 residue), wHsp16.9 (8 residues), αA-

crystallin (12 residues), or αB-crystallin (14 residues). Notably, replacement of Pro182 with Leu in Hsp27, which is located at the hinge between the IXI motif and the last 24 residues, is the only known mutation outside of the α-crystallin domain that leads to a human disease.[10]

It seems clear that the role of the C-terminal sequence is associated with its hydrophilic composition and its position within the Hsp27 quaternary structure. Cryo–EM[51,52] and NMR experiments[23] confirm the flexibility of this region and its exposure to the solvent when the protein forms large assemblies. Removal of the C-terminus inhibits unfolding of the Hsp27 polypeptide chain as seen by circular dichroism and eliminates the thermally-induced increase in subunit exchange observed by FRET experiments, suggesting that the mobility of this region contributes to initiation of oligomer dissociation and promotes protein unfolding. Thermally induced disruption of quaternary structure has been linked previously to chaperone activity of Hsp27.[39,53] It is possible that the increase in thermal energy resulting from heat shock induces greater conformational variation in the exposed C-terminal sequence and thereby leads to increased rates of subunit exchange among the larger oligomers as indicated by the FRET results that show that subunit exchange of the Δ182–205 variant does not increase with increasing temperature as observed for wild-type Hsp27.

Finally, although the IXI motif presumably binds to the β4–β8 groove of an α-crystallin domain, to which domain it binds within an oligomeric assembly will depend on a number of factors including the length of the N-terminal sequence and the conformation of the flexible C-terminal sequence. In fact, removing the 24 C-terminal residues, locks the protein into a temperature-independent quaternary structure distinct from the temperature-dependent quaternary structure of the wild-type protein. Interestingly, both α-crystallins contain a palindromic sequence around the central proline (i.e., *E*/*D*–R–X–**I**–P–**V/I**–R–*E*/*D*) with two arginines in this sequence that form important hydrogen bonds in the β4–β8 groove.[28] Hsp27 lacks this palindromic sequence and the argininyl residues while it has an extra isoleucine and phenylalanine flanked by the acidic residues also found in α-crystallin (i.e., ^{178}*E*–**I**–T–**I**–P–**V**–T–**F**–*E*^{186}). We note that the IXI domain in this conserved region of Hsp27 has the ambiguous sequence ITIPV that could function as an IXI domain in one of two ways. Specifically, this sequence could bind to another subunit by means of either the ITI or IPV sequences in a manner that varies with the size of the oligomer. Previous studies on the IXI motif of αA/B-crystallin also led to the conclusion that this region of the protein is responsible for various oligomeric assemblies.[28,40]

A model for Hsp27 chaperone activity

Wild-type Hsp27 fully inhibits insulin unfolding at a ratio much smaller than 1:1 (insulin:Hsp27 subunit), and one Hsp27 oligomer can bind more than one molecule of insulin at a time. The crystal structures of wHsp16.9, MjHsp16.5, and Tsp36 all indicate that upon formation of the large oligomer, an extensive hydrophobic surface of each monomer is buried in the final assembly. Moreover, Langanowski *et al.*[28] have reported that there are at least three possible ways in which two α-crystallin domains can interact to form dimers through the edge strands of the antiparallel β-sheet, increasing the number of possible oligomers formed as well as the nature of the hydrophobic patches that are exposed upon dissociation of the oligomers. Repeated dissociation and re-association presumably exposes similar hydrophobic patches on the surface of Hsp27 that result in recognition and interaction with unfolding peptides in a non-specific manner. The correlation of increased oligomer size and chaperone activity reported previously for Hsp27 at elevated temperature with the thermally-enhanced rate of subunit exchange observed in this study is consistent with this hypothesis. In addition, a recent study of dodecameric Hsp18.1 indicates that the oligomeric state is not its active form. As with Hsp27, this protein both dissociates into smaller oligomers and forms larger oligomers at elevated temperatures to bind to unfolding luciferase. Mass spectrometry of Hsp18.1-luciferase complexes indicates the formation of as many as 300 combinations of chaperone–substrate complexes that vary in both the size of the Hsp18.1 oligomer and the number of substrate molecules bound.[54]

Although subunit exchange may be necessary for chaperone activity, it is not sufficient. In this study, we observed that the Δ1–14 Hsp27 variant exhibits efficient subunit exchange but no chaperone activity, suggesting a crucial role for the 14 N-terminal residues in direct binding to unfolding proteins and/or in the formation of larger oligomers. Such a role is consistent with cryo-EM studies of Hsp25 and Hsp26 and with mass spectrometry data for Hsp18.1 indicating that these proteins bind substrate to form complexes at least as large as those formed by each protein in the absence of substrate.[54,55]

The lack of a flexible C-terminal sequence in the Δ182–205 variant inhibits chaperone activity only at low temperature (20 °C) while activity persists at heat shock temperature (40 °C). Interestingly, light scattering of unfolding insulin at 20 °C is greater in the presence of the Δ182–205 variant than in its absence, probably as a result of the formation of insoluble Δ182–205/insulin complexes that scatter light more than does unfolding insulin alone. This possibility is consistent with the hypothesis that the C-terminal sequence promotes subunit exchange and increases solubility at low temperature and that the

lack of this flexible sequence at 20 °C inhibits subunit exchange as well as reduces the solubility of the complex, thereby inhibiting chaperone activity.

In general, it is likely that the ability to dissociate, expose hydrophobic patches capable of quickly capturing unfolding proteins and then reassociate into large, stable and soluble oligomers is a common feature of small, ATP-independent, mammalian heat shock proteins.

Conclusions

Some fundamental characteristics of the complex mechanism by which Hsp27 self-associates and promotes the solubility of unfolding proteins are now apparent that expand on the established role of the α-crystallin domain. Specifically, we propose a model in which (a) the helical fold predicted for the N-terminal sequence can engage in multiple interactions with similar regions of neighboring monomers that are essential for the formation of larger oligomers at ambient and elevated temperatures and for chaperone activity but not for subunit exchange; (b) the C-terminal sequence undergoes a temperature-dependent conformational change that is essential for the formation of larger oligomers at elevated temperature and for initiation of dissociation and subunit exchange; and (c) both subunit exchange and reassociation to form larger oligomers are required for Hsp27 chaperone activity. Hsp27–substrate complexes may exhibit a polydispersity as complex as that observed for Hsp18.1.[54] In this case, the 24-mer observed under standard experimental conditions is simply a reservoir of Hsp27 that requires thermal activation as the result of cellular stress to promote dissociation, binding, and reassociation with protein substrates. Further studies are required to define the stoichiometry of Hsp27–substrate interaction that is involved in chaperone activity and to evaluate the dependence of this stoichiometry on the size and structure of the substrate.

Materials and Methods

Protein purification

Expression and purification of wild-type human Hsp27 and the three deletion variants Δ1–14 Hsp27, Δ1–24 Hsp27, Δ182–205 Hsp27 (Fig. 1) were performed as described previously.[21]

Sedimentation velocity analyses

The solution densities and partial specific volumes of the proteins studied here were calculated with the program SEDNTERP.[56] Monomer molecular weights and molar absorptivities were calculated from the amino acid sequences with the program ProtParam at the ExPASy web site.[57] Sedimentation velocity experiments were conducted at 40 °C with a Beckman Optima XL–I analytical ultracentrifuge[30] and with protein prepared in Tris–HCl buffer (20 m*M*, pH 8.4, 100 m*M* NaCl). This pH was used to permit comparison of current results with our published results. Most of the other experiments were conducted at pH 6.7–7.7 with the assumption that protein stability and folding are unchanged over this range of pH as observed for the wild-type protein.[21] In this regard, we note that at 30 and 40 °C, the pH of the Tris buffer is expected to decrease from 8.4 (at 20 °C) to 7.9 and 7.6, respectively.[58] These latter values are, in fact, closer to the pH at which the thermal stability, chaperone activity, and FRET were measured. Data were analyzed with the program SEDPHAT as previously reported.[21,30]

Thermal stability measurements

Thermal denaturation of Hsp27 variants (10 μ*M*) was studied by monitoring ellipticity at 219 nm (phosphate buffer (10 m*M*, pH 6.7 or 7.7); 25–90 °C (1 °C/min)) with a Jasco Model 810 spectropolarimeter equipped with a Peltier device operated under computer control. UV CD spectra were recorded at 25 °C before and after unfolding. Phosphate buffer was used rather than Tris-HCl as the latter does not buffer in this pH range, it has a pK_a that is highly dependent on temperature, and it interferes with CD measurements.

Chaperone activity assays

Chaperone activity was measured by monitoring the DTT-induced aggregation of human insulin in the absence and presence of Hsp27 variants.[30]

Fluorescent labeling of Hsp27

Wild-type Hsp27 and selected variants were labeled[20,32] at the unique cysteinyl residue, Cys137, with either 4-aceto-4′-((iodoacetyl)amino) stilbene-2,2′-disulfonic acid (AIAS, $\lambda_{ex} = 329$ nm, $\lambda_{em} = 408$ nm) (Invitrogen) or lucifer yellow iodoacetamide (LYI, $\lambda_{ex} = 426$ nm, $\lambda_{em} = 531$ nm) (Invitrogen). The extinction coefficients used to determine the labeling efficiency were 39,000 M^{-1} cm^{-1} for AIAS and 11,000 M^{-1} cm^{-1} for LYI as indicated by the supplier.

FRET measurements

Fluorescence resonance energy transfer was used to determine the rate of subunit exchange of wild-type Hsp27 and variants as a function of temperature.[20,32] Following preparation of Hsp27 modified with the fluorescent labels AIAS and LYI, subunit exchange was initiated by mixing equimolar (5 μ*M* final) AIAS-labeled and LYI-labeled protein in a quartz cuvette (1 cm path length) in a total volume of 160 μL (50 m*M* sodium phosphate (pH 7.5), 100 m*M* NaCl, 2 mM DTT). The excitation wavelength was 335 nm, and quenching was monitored by measuring fluorescence emission (412 nm) with a Cary Eclipse spectrofluorometer. Protein was incubated at the desired temperature for at least 15 min prior to

each experiment and was maintained at constant temperature with a Peltier device. The rate of subunit exchange was calculated from the equation $F(t) = y_0 + Ae^{-x/t_{mrt}}$, where *F(t)* is the fluorescence intensity at 412 nm and t_{mrt} is the mean reaction time.[59] The rate constant k, which is equal to $1/t_{mrt}$, was determined by nonlinear regression analysis of the data using a first order or bi-exponential decay function (Origin 7.0, OriginLabs). The activation energy (E_a) for subunit exchange was determined from Arrhenius plots ($1/T$ (K^{-1}) *vs.* $\ln(k)$). The data were analyzed by a linear least squares fit to $y = A + Bx$ where $A = \Delta S/R$ and $B = -\Delta H/R$ (R = gas constant), and the activation energy was calculated from the relationship $E_a = \Delta H + RT$.

Acknowledgments

We thank Dr. Louise Creagh for assistance in use of the analytical ultracentrifuge and Prof. J. Landry (Centre de Recherché en Cancerologie de l'Université Laval, Quebec) for providing the gene encoding human Hsp27. The analytical ultracentrifuge was operated by the UBC Laboratory of Molecular Biophysics through support from a Michael Smith Foundation for Health Research Infrastructure Grant.

References

1. Kampinga HH, Hageman J, Vos MJ, Kubota H, Tanguay RM, Bruford EA, Cheetham ME, Chen B, Hightower LE (2009) Guidelines for the nomenclature of the human heat shock proteins. Cell Stress Chaperones 14:105–111.
2. Jakob U, Gaestel M, Engel K, Buchner J (1993) Small heat shock proteins are molecular chaperones. J Biol Chem 268:1517–1520.
3. Garrido C, Bruey JM, Fromentin A, Hammann A, Arrigo AP, Solary E (1999) HSP27 inhibits cytochrome *c*-dependent activation of procaspase-9. Faseb J 13: 2061–2070.
4. Pivovarova AV, Chebotareva NA, Chernik IS, Gusev NB, Levitsky DI (2007) Small heat shock protein Hsp27 prevents heat-induced aggregation of F-actin by forming soluble complexes with denatured actin. FEBS J 274:5937–5948.
5. Gusev NB, Bogatcheva NV, Marston SB (2002) Structure and properties of small heat shock proteins (sHsp) and their interaction with cytoskeleton proteins. Biochemistry (Mosc) 67:511–519.
6. Garrido C, Gurbuxani S, Ravagnan L, Kroemer G (2001) Heat shock proteins: endogenous modulators of apoptotic cell death. Biochem Biophys Res Commun 286:433–442.
7. Garrido C (2002) Size matters: of the small HSP27 and its large oligomers. Cell Death Differ 9:483–485.
8. Schmitt E, Gehrmann M, Brunet M, Multhoff G, Garrido C (2007) Intracellular and extracellular functions of heat shock proteins: repercussions in cancer therapy. J Leukoc Biol 81:15–27.
9. Garrido C, Fromentin A, Bonnotte B, Favre N, Moutet M, Arrigo AP, Mehlen P, Solary E (1998) Heat shock protein 27 enhances the tumorigenicity of immunogenic rat colon carcinoma cell clones. Cancer Res 58:5495–5499.
10. Evgrafov OV, Mersiyanova I, Irobi J, Van Den Bosch L, Dierick I, Leung CL, Schagina O, Verpoorten N, Van Impe K, Fedotov V, Dadali E, Auer-Grumbach M, Windpassinger C, Wagner K, Mitrovic Z, Hilton-Jones D, Talbot K, Martin JJ, Vasserman N, Tverskaya S, Polyakov A, Liem RK, Gettemans J, Robberecht W, De Jonghe P, Timmerman V (2004) Mutant small heat-shock protein 27 causes axonal Charcot-Marie-Tooth disease and distal hereditary motor neuropathy. Nat Genet 36:602–606.
11. Tang B, Liu X, Zhao G, Luo W, Xia K, Pan Q, Cai F, Hu Z, Zhang C, Chen B, Zhang F, Shen L, Zhang R, Jiang H (2005) Mutation analysis of the small heat shock protein 27 gene in chinese patients with Charcot-Marie-Tooth disease. Arch Neurol 62:1201–1207.
12. Kijima K, Numakura C, Goto T, Takahashi T, Otagiri T, Umetsu K, Hayasaka K (2005) Small heat shock protein 27 mutation in a Japanese patient with distal hereditary motor neuropathy. J Hum Genet 50:473–476.
13. Aquino DA, Capello E, Weisstein J, Sanders V, Lopez C, Tourtellotte WW, Brosnan CF, Raine CS, Norton WT (1997) Multiple sclerosis: altered expression of 70- and 27-kDa heat shock proteins in lesions and myelin. J Neuropathol Exp Neurol 56:664–672.
14. Stege GJ, Renkawek K, Overkamp PS, Verschuure P, van Rijk AF, Reijnen-Aalbers A, Boelens WC, Bosman GJ, de Jong WW (1999) The molecular chaperone αB-crystallin enhances amyloid β neurotoxicity. Biochem Biophys Res Commun 262:152–156.
15. Renkawek K, Stege GJ, Bosman GJ (1999) Dementia, gliosis and expression of the small heat shock proteins hsp27 and αB-crystallin in Parkinson's disease. Neuroreport 10:2273–2276.
16. Head MW, Corbin E, Goldman JE (1993) Overexpression and abnormal modification of the stress proteins αB-crystallin and HSP27 in Alexander disease. Am J Pathol 143:1743–1753.
17. Iwaki T, Iwaki A, Tateishi J, Sakaki Y, Goldman JE (1993) αB-crystallin and 27-kd heat shock protein are regulated by stress conditions in the central nervous system and accumulate in Rosenthal fibers. Am J Pathol 143:487–495.
18. Kato S, Hirano A, Umahara T, Llena JF, Herz F, Ohama E (1992) Ultrastructural and immunohistochemical studies on ballooned cortical neurons in Creutzfeldt-Jakob disease: expression of αB-crystallin, ubiquitin and stress-response protein 27. Acta Neuropathol (Berl) 84:443–448.
19. Caspers GJ, Leunissen JA, de Jong WW (1995) The expanding small heat-shock protein family, and structure predictions of the conserved "α-crystallin domain". J Mol Evol 40:238–248.
20. Bova MP, McHaourab HS, Han Y, Fung BK (2000) Subunit exchange of small heat shock proteins. Analysis of oligomer formation of α-crystallin and Hsp27 by fluorescence resonance energy transfer and site-directed truncations. J Biol Chem 275:1035–1042.
21. Lelj-Garolla B, Mauk AG (2005) Self-association of a small heat shock protein. J Mol Biol 345:631–642.
22. Lambert H, Charette SJ, Bernier AF, Guimond A, Landry J (1999) HSP27 multimerization mediated by phosphorylation-sensitive intermolecular interactions at the amino terminus. J Biol Chem 274:9378–9385.
23. Carver JA, Esposito G, Schwedersky G, Gaestel M (1995) ^{1}H NMR spectroscopy reveals that mouse Hsp25 has a flexible *C*-terminal extension of 18 amino acids. FEBS Lett 369:305–310.
24. Kim KK, Kim R, Kim SH (1998) Crystal structure of a small heat-shock protein. Nature 394:595–599.
25. van Montfort RL, Basha E, Friedrich KL, Slingsby C, Vierling E (2001) Crystal structure and assembly of a

eukaryotic small heat shock protein. Nat Struct Biol 8: 1025–1030.
26. Stamler R, Kappe G, Boelens W, Slingsby C (2005) Wrapping the α-crystallin domain fold in a chaperone assembly. J Mol Biol 353:68–79.
27. Bagneris C, Bateman OA, Naylor CE, Cronin N, Boelens WC, Keep NH, Slingsby C (2009) Crystal structures of α-crystallin domain dimers of αB-crystallin and Hsp20. J Mol Biol 392:1242–1252.
28. Laganowsky A, Benesch JL, Landau M, Ding L, Sawaya MR, Cascio D, Huang Q, Robinson CV, Horwitz J, Eisenberg D (2010) Crystal structures of truncated αA and αB crystallins reveal structural mechanisms of polydispersity important for eye lens function. Protein Sci 19:1031–1043.
29. Vos MJ, Hageman J, Carra S, Kampinga HH (2008) Structural and functional diversities between members of the human HSPB, HSPH, HSPA, and DNAJ chaperone families. Biochemistry 47:7001–7011.
30. Lelj-Garolla B, Mauk AG (2006) Self-association and chaperone activity of Hsp27 are thermally activated. J Biol Chem 281:8169–8174.
31. Dudich IV, Zav'yalov VP, Pfeil W, Gaestel M, Zav'yalova GA, Denesyuk AI, Korpela T (1995) Dimer structure as a minimum cooperative subunit of small heat-shock proteins. Biochim Biophys Acta 1253:163–168.
32. Bova MP, Ding LL, Horwitz J, Fung BK (1997) Subunit exchange of αA-crystallin. J Biol Chem 272:29511–29517.
33. Fu X, Liu C, Liu Y, Feng X, Gu L, Chen X, Chang Z (2003) Small heat shock protein Hsp16.3 modulates its chaperone activity by adjusting the rate of oligomeric dissociation. Biochem Biophys Res Commun 310:412–420.
34. Jiao W, Qian M, Li P, Zhao L, Chang Z (2005) The essential role of the flexible termini in the temperature-responsiveness of the oligomeric state and chaperone-like activity for the polydisperse small heat shock protein IbpB from *Escherichia coli*. J Mol Biol 347:871–884.
35. Usui K, Hatipoglu OF, Ishii N, Yohda M (2004) Role of the N-terminal region of the crenarchaeal sHsp, StHsp14.0, in thermal-induced disassembly of the complex and molecular chaperone activity. Biochem Biophys Res Commun 315:113–118.
36. Bova MP, Huang Q, Ding L, Horwitz J (2002) Subunit exchange, conformational stability, and chaperone-like function of the small heat shock protein 16.5 from *Methanococcus jannaschii*. J Biol Chem 277:38468–38475.
37. Kundu M, Sen PC, Das KP (2007) Structure, stability, and chaperone function of αA-crystallin: role of N-terminal region. Biopolymers 86:177–192.
38. Liao JH, Lee JS, Chiou SH (2002) C-terminal lysine truncation increases thermostability and enhances chaperone-like function of porcine αB-crystallin. Biochem Biophys Res Commun 297:309–316.
39. Pasta SY, Raman B, Ramakrishna T, Rao Ch M (2003) Role of the conserved SRLFDQFFG region of α-crystallin, a small heat shock protein. Effect on oligomeric size, subunit exchange, and chaperone-like activity. J Biol Chem 278:51159–51166.
40. Pasta SY, Raman B, Ramakrishna T, Rao Ch M (2004) The IXI/V motif in the C-terminal extension of α-crystallins: alternative interactions and oligomeric assemblies. Mol Vis 10:655–662.
41. Kim SJ, Jeong DG, Chi SW, Lee JS, Ryu SE (2001) Crystal structure of proteolytic fragments of the redox-sensitive Hsp33 with constitutive chaperone activity. Nat Struct Biol 8:459–466.
42. Haslbeck M, Ignatiou A, Saibil H, Helmich S, Frenzl E, Stromer T, Buchner J (2004) A domain in the N-terminal part of Hsp26 is essential for chaperone function and oligomerization. J Mol Biol 343:445–455.
43. Plater ML, Goode D, Crabbe MJ (1996) Effects of site-directed mutations on the chaperone-like activity of αB-crystallin. J Biol Chem 271: 28558–28566.
44. Theriault JR, Lambert H, Chavez-Zobel AT, Charest G, Lavigne P, Landry J (2004) Essential role of the NH_2-terminal WD/EPF motif in the phosphorylation-activated protective function of mammalian Hsp27. J Biol Chem 279:23463–23471.
45. Carver JA, Aquilina JA, Truscott RJ, Ralston GB (1992) Identification by ^{1}H NMR spectroscopy of flexible *C*-terminal extensions in bovine lens α-crystallin. FEBS Lett 311:143–149.
46. Lindner RA, Carver JA, Ehrnsperger M, Buchner J, Esposito G, Behlke J, Lutsch G, Kotlyarov A, Gaestel M (2000) Mouse Hsp25, a small shock protein. The role of its C-terminal extension in oligomerization and chaperone action. Eur J Biochem 267:1923–1932.
47. Guo Z, Cooper LF (2000) An N-terminal 33-amino-acid-deletion variant of hsp25 retains oligomerization and functional properties. Biochem Biophys Res Commun 270:183–189.
48. Li Y, Schmitz KR, Salerno JC, Koretz JF (2007) The role of the conserved COOH-terminal triad in αA-crystallin aggregation and functionality. Mol Vis 13: 1758–1768.
49. Studer S, Obrist M, Lentze N, Narberhaus F (2002) A critical motif for oligomerization and chaperone activity of bacterial α-heat shock proteins. Eur J Biochem 269: 3578–3586.
50. Chen J, Feige MJ, Franzmann TM, Bepperling A, Buchner J (2010) Regions outside the α-crystallin domain of the small heat shock protein Hsp26 are required for its dimerization. J Mol Biol 398:122–131.
51. Haley DA, Horwitz J, Stewart PL (1998) The small heat-shock protein, αB-crystallin, has a variable quaternary structure. J Mol Biol 277:27–35.
52. Haley DA, Bova MP, Huang QL, McHaourab HS, Stewart PL (2000) Small heat-shock protein structures reveal a continuum from symmetric to variable assemblies. J Mol Biol 298:261–272.
53. Smulders R, Carver JA, Lindner RA, van Boekel MA, Bloemendal H, de Jong WW (1996) Immobilization of the C-terminal extension of bovine αA-crystallin reduces chaperone-like activity. J Biol Chem 271: 29060–29066.
54. Stengel F, Baldwin AJ, Painter AJ, Jaya N, Basha E, Kay LE, Vierling E, Robinson CV, Benesch JL (2010) Quaternary dynamics and plasticity underlie small heat shock protein chaperone function. Proc Natl Acad Sci USA 107:2007–2012.
55. Stromer T, Ehrnsperger M, Gaestel M, Buchner J (2003) Analysis of the interaction of small heat shock proteins with unfolding proteins. J Biol Chem 278: 18015–18021.
56. Laue TM, Shah BD, Ridgeway TM, Pelletier SL, Computer-aided interpretation of analytical sedimentation data for proteins. In: Harding S, Rowe A, Horton J, Eds. (1992) Analytical ultracentrifugation in biochemistry and polymer science. Cambridge: Royal Society of Chemistry, pp 90–125.
57. Gill SC, von Hippel PH (1989) Calculation of protein extinction coefficients from amino acid sequence data. Anal Biochem 182:319–326.
58. Goldberg RN, Kishore N, Lennen RM (2002) Thermodynamic quantities for the ionization reactions of buffers. J Phys Chem Ref Data 31:232–370.
59. Espenson JH (1981) Chemical kinetics and reaction mechanisms, McGraw-Hill Book Company.